J Stat Phys (2010) 140: 934–947
DOI 10.1007/s10955-010-0025-6

Dynamic Phase Transitions and Compensation Temperatures in a Mixed Spin-3/2 and Spin-5/2 Ising System

Bayram Deviren · Mustafa Keskin

Received: 5 April 2010 / Accepted: 9 July 2010 / Published online: 30 July 2010

Abstract We examine the dynamic phase transitions and the dynamic compensation temperatures, within a mean-field approach, in the mixed spin-3/2 and spin-5/2 Ising system with a crystal-field interaction under a time-varying magnetic field on a hexagonal lattice by using Glauber-type stochastic dynamics. The model system consists of two interpenetrating sublattices with $\sigma = 3/2$ and $S = 5/2$. The Hamiltonian model includes intersublattice, intrasublattice, and crystal-field interactions. The intersublattice interaction is considered antiferromagnetic and to be a simple but interesting model of a ferrimagnetic system. We employ the Glauber transition rates to construct the mean-field dynamic equations, and we solve these equations in order to find the phases in the system. We also investigate the thermal behavior of the dynamic sublattice magnetizations and the dynamic total magnetization to obtain the dynamic phase transition points and compensation temperatures as well as to characterize the nature (continuous and discontinuous) of transitions. We also calculate the dynamic phase diagrams including the compensation temperatures in five different planes. According to the values of Hamiltonian parameters, five different fundamental phases, three different mixed phases, and six different types of compensation behaviors in the Néel classification nomenclature exist in the system.

Keywords Mixed-spin Ising system · Dynamic phase transitions · Dynamic compensation temperature · Dynamic phase diagrams · Glauber-type stochastic dynamics

B. Deviren · M. Keskin (✉)
Institute of Science, Erciyes University, 38039 Kayseri, Turkey
e-mail: keskin@erciyes.edu.tr

B. Deviren
Department of Physics, Nevsehir University, 50300 Nevşehir, Turkey

M. Keskin
Department of Physics, Erciyes University, 38039 Kayseri, Turkey

1 Introduction

Mixed spin Ising systems provide good models for investigating the ferrimagnetic materials which are currently the subject of a great deal of interest due to their great potential for technological applications, as well as for academic research. These systems also supply simple models for the study of molecular-based ferrimagnets which could be potentially useful materials for magneto-optical recordings. Moreover, under certain conditions, these systems can have a compensation temperature where the total magnetization vanishes below the critical temperature. The existence of compensation temperatures is of great technological importance since at this point only a small driving field is required to change the sign of the total magnetization.

Many combinations of mixed-spin Ising systems, such as spins (1/2, 1), spins (1/2, 3/2), spins (1, 3/2), spins (1, 2), etc., have been studied by a variety of techniques in equilibrium statistical physics. The exact solutions of some of the mixed-spin Ising systems have also been studied on a honeycomb lattice, a bathroom-tile, diced lattices, a Bethe lattice, two-fold Cayley tree and several decorated planer lattices. Half-integer spin systems are more exciting for a number of reasons. First, they can show multicritical behavior or a magnetoelastic transition or instability, and second they are less studied [1]. The simplest and most studied half-integer mixed-spin Ising system is spins (1/2, 3/2) which has been extensively studied (see [2–12] and references therein). Another half-integer mixed-spin Ising system which has been studied is spins (1/2, 5/2) but this has been investigated less extensively than spins (1/2, 3/2) [13, 14]. Another possible half-integer mixed-spin Ising system is spins (3/2, 5/2) which is the highest mixed-spin Ising system and less explored the mixed system. An early attempt to study the mixed spin-3/2 and spin-5/2 ferrimagnetic Ising model was made within the framework of the effective-field theory (EFT) [15], where the phase diagrams and the internal energy of the system on the honeycomb lattice with interlayer coupling was investigated. The system has also been investigated on the Bethe lattice by using exact recursion relations, and it was found that it exhibits one or two compensation temperatures depending on the values of the crystal fields [16]. It was also found that the system on the Bethe lattice undergoes first- and second-order phase transitions, but does not give any tricritical points. The mixed spin-3/2 and spin-5/2 Ising model on the two-fold Cayley tree was studied by means of exact recursion relations, and a first- and second-order phase transitions were found [17]. Recently, the ground state phase diagrams for the mixed Ising 3/2 and 5/2 spin model were investigated extensively [18].

On the other hand, many complicated high spin magnets have been synthesized [19]; hence the equilibrium and nonequilibrium behaviors of high mixed-spin Ising systems, such as spins (3/2, 5/2) should be investigated in detail. Moreover, a variety of critical points can be found and more phases are possible for larger spins, e.g. compare the results of spins (1/2, 1) [20] with spins (1, 3/2) [21] and with spins (1, 5/2) [22]. We should also mention that the mixed spins (3/2, 5/2) model appears to be convenient to the understanding of particular biological compounds. For example, some experimental studies point out that a mixed of 3/2 and 5/2 spins is behind the unusual magnetic properties of certain types of ferric heme proteins known as ferricytochromes c′ [23–26]. Heme proteins are used as a synthetic base to design novel biomaterials with great potential applications in optical communications, and are considered as the base for nanoporous catalytic materials [27], besides their important role in oxygen transport by blood. Therefore, the aim of this paper is to study the nonequilibrium properties of the kinetic mixed spin-3/2 and spin-5/2 ferrimagnetic Ising system with a crystal-field interaction under a time-varying magnetic field on a hexagonal lattice by using the Glauber-type stochastic dynamics [28]. In particular, we calculate the dynamic phase transition temperatures, and present the dynamic phase diagrams;

we also study the dynamic compensation behaviors. For these purposes, first we employ the Glauber transition rates to construct the mean-field dynamic equations and solve these equations in order to find the phases in the system. Then we investigate the thermal behavior of the dynamic sublattice magnetizations and dynamic total magnetization to obtain the dynamic phase transition points and dynamic compensation temperatures as well as to characterize the nature (continuous or discontinuous) of the transitions. We also present the dynamic phase diagrams including the compensation temperatures in five different planes.

It is worthwhile mentioning that in recent years, the dynamic phase transition has become an interesting field of researches in magnetic systems, theoretically (see [20–22], [29–32] and references therein), and experimentally in amorphous YBaCuO films [33], ultrathin Co films on a Cu(001) surface [34], ferroic systems (ferromagnets, ferroelectrics and ferroelastics) with pinned domain walls [35], cuprate superconductors [36], $[Co/Pt]_3$ magnetic multilayers [37], and polyethylene naphthalate (PEN) nanocomposites [38]. On the other hand, the increasing interest in compensation behaviors is mainly related to the potential technological applications of these systems in the area of thermomagnetic recording [39–42]. The presence of the compensation temperature in mixed spin Ising systems has been studied by well-known methods in equilibrium statistical physics (see [43] and references therein). Moreover, the existence of the dynamic compensation temperatures in kinetic mixed-spin Ising systems with spins (1/2, 1) [44–46], with spins (1/2, 3/2) [47] and with spins (2, 5/2) [48] has also been investigated. Finally, it is worthwhile mentioning that the compensation temperature has been observed experimentally in different systems [49, 50].

The rest of the paper is organized as follows. In Sect. 2, the model is presented and the derivation of the mean-field dynamic equations of motion is given by using a Glauber-type stochastic dynamics in the presence of a time-dependent oscillating external magnetic field. In Sect. 3, the numerical results for the average sublattice magnetizations, dynamic sublattice magnetizations, dynamic total magnetization and dynamic phase diagrams are studied in detail. Finally, a summary and conclusion are given in the last section.

2 Model and Formulations

We consider a mixed spin-3/2 and spin-5/2 Ising system on a hexagonal lattice under the oscillating magnetic field. The model consists of two interpenetrating sublattices with σ and S spins; hence the two different types of spins are described by Ising variables, which can take the values $\sigma = \pm 3/2, \pm 1/2$ and $S = \pm 5/2, \pm 3/2, \pm 1/2$. The Hamiltonian model for the system is

$$H = -J_a \sum_{\langle ij \rangle} \sigma_i \sigma_j - J_b \sum_{\langle ij \rangle} S_i S_j - J_{ab} \sum_{\langle ij \rangle} \sigma_i S_j - \Delta \left(\sum_i \sigma_i^2 + \sum_j S_j^2 \right) - H \left(\sum_i \sigma_i + \sum_j \mathrm{S}_j \right), \tag{1}$$

where the summation index $\langle ij \rangle$ denotes a summation over all pairs of nearest-neighbor spins. J_a, J_b and J_{ab} are the exchange couplings between the nearest-neighbor pairs of spins σ-σ, S-S and σ-S, respectively. J_{ab} interaction is restricted to the z_1 nearest-neighbor pair of spins, that $z_1 = 4$, and J_a and J_b are restricted to the coordination numbers of z_2 and z_3, respectively, in which $z_2 = z_3 = 2$. The parameter J_{ab} will be taken as negative in all subsequent analyses, that is, the intersublattice coupling is antiferromagnetic and is a

simple but interesting model of a ferrimagnetic system. Δ is the crystal-field interaction or a single-ion anisotropy constant, and H is a time-dependent external oscillating magnetic field: $H(t) = H_0 \cos(wt)$, with H_0 and $w = 2\pi\nu$ being the amplitude and the angular frequency of the oscillating field, respectively. The system is in contact with an isothermal heat bath at an absolute temperature T_A.

Now, we apply the Glauber-type stochastic dynamics [28] to obtain the set of mean-field dynamic equation. Thus, the system evolves according to the Glauber-type stochastic process at a rate of $1/\tau$ transitions per unit time; hence the frequency of spin flipping, f, is $1/\tau$. Leaving the S spins fixed, we define $P^{\sigma}(\sigma_1, \sigma_2, \ldots, \sigma_N; t)$ as the probability that the system has the σ-spin configuration, $\sigma_1, \sigma_2, \ldots, \sigma_N$, at time t, also, by leaving the σ spins fixed, we define $P^{S}(S_1, S_2, \ldots, S_N; t)$ as the probability that the system has the S-spin configuration, $S_1, S_2, \ldots, S_N$, at time t. Then, we calculate $W_i^{\sigma}(\sigma_i \to \sigma_i')$ and $W_j^{S}(S_j \to S_j')$, the probabilities per unit time that the ith σ spin changes from σ_i to σ_i' (while the S spins are momentarily fixed) and the jth S spin changes from S_j to S_j' (while the σ spins are momentarily fixed), respectively. Thus, if the S spins are momentarily fixed, the master equation for the σ spins can be written as

$$\frac{d}{dt}P^{\sigma}(\sigma_1, \sigma_2, \ldots, \sigma_N; t) = -\sum_i \left(\sum_{\sigma_i \neq \sigma_i'} W_i^{\sigma}\left(\sigma_i \to \sigma_i'\right) \right) P^{\sigma}(\sigma_1, \sigma_2, \ldots, \sigma_i, \ldots \sigma_N; t) + \sum_i \left(\sum_{\sigma_i \neq \sigma_i'} W_i^{\sigma}\left(\sigma_i' \to \sigma_i\right) \right) P^{\sigma}\left(\sigma_1, \sigma_2, \ldots, \sigma_i', \ldots \sigma_N; t\right), \quad (2)$$

where $W_i^{\sigma}(\sigma_i \to \sigma_i')$ is the probability per unit time that the ith spin changes from the value σ_i to σ_i'. Since the system is in contact with a heat bath at absolute temperature T_A, each spin can change from the value σ_i to σ_i' with the probability per unit time;

$$W_i^{\sigma}\left(\sigma_i \to \sigma_i'\right) = \frac{1}{\tau} \frac{\exp[-\beta \Delta E^{\sigma}(\sigma_i \to \sigma_i')]}{\sum_{\sigma_i'} \exp[-\beta \Delta E^{\sigma}(\sigma_i \to \sigma_i')]}, \quad (3)$$

where $\beta = 1/k_B T_A$, k_B is the Boltzmann constant and $k_B = 1$ is taken, $\sum_{\sigma_i'}$ is the sum over the four possible values of $\sigma_i' = \pm 3/2, \pm 1/2$, and

$$\Delta E^{\sigma}\left(\sigma_i \to \sigma_i'\right) = -\left(\sigma_i' - \sigma_i\right)\left(J_a \sum_j \sigma_j + J_{ab} \sum_j S_j + H \right) - \left[\left(\sigma_i'\right)^2 - (\sigma_i)^2\right]\Delta, \quad (4)$$

gives the change in the system's energy when the σ_i-spin changes. The probabilities satisfy the detailed balance condition. Since $W_i^{\sigma}(\sigma_i \to \sigma_i')$ does not depend on the value σ_i, we can write $W_i^{\sigma}(\sigma_i \to \sigma_i') = W_i^{\sigma}(\sigma_i')$, then the master equation becomes

$$\frac{d}{dt}P^{\sigma}(\sigma_1, \sigma_2, \ldots, \sigma_N; t) = -\sum_i \left(\sum_{\sigma_i \neq \sigma_i'} W_i^{\sigma}\left(\sigma_i'\right) \right) P^{\sigma}(\sigma_1, \sigma_2, \ldots, \sigma_i, \ldots, \sigma_N; t) + \sum_i W_i^{\sigma}(\sigma_i) \left(\sum_{\sigma_i \neq \sigma_i'} P^{A}\left(\sigma_1, \sigma_2, \ldots, \sigma_i', \ldots, \sigma_N; t\right) \right). \quad (5)$$

Since the sum of the probabilities is normalized to one, by multiplying both sides of (5) by σ_k and taking the average and finally by using a mean-field approach, we obtain the first

mean-field dynamic equation for the σ spins:

$$\Omega\frac{d}{d\xi}m_\sigma = -m_\sigma + \frac{3\sinh(3\frac{a_1}{T})\exp(\frac{d}{T}) + \sinh(\frac{a_1}{T})\exp(-\frac{d}{T})}{2\cosh(3\frac{a_1}{T})\exp(\frac{d}{T}) + \cosh(\frac{a_1}{T})\exp(-\frac{d}{T})}, \tag{6}$$

where $a_1 = z_1 m_S + \frac{J_a}{|J_{ab}|} z_2 m_\sigma + h_0\cos(\xi), m_\sigma = \langle\sigma\rangle,\ m_s = \langle S\rangle,\ T = \frac{k_B T_A}{|J_{ab}|},\ d = \frac{\Delta}{|J_{ab}|}$, $h_0 = \frac{H_0}{|J_{ab}|}, \xi = wt$ and $\Omega = \tau w$.

Now assuming that the σ-spins remain momentarily fixed and that the S-spins change, we obtain the mean-field dynamical equation for the S-spins by using the similar calculations as before, except we take $S_{j'} = \pm 5/2, \pm 3/2, \pm 1/2$ instead of $\sigma_{i'} = \pm 3/2, \pm 1/2$. The second mean-field dynamic equation for the S spins is obtained as

$$\Omega\frac{d}{d\xi}m_S = -m_S + \frac{5\exp(\frac{2d}{T})\sinh(\frac{5a_2}{2T}) + 3\exp(-2\frac{d}{T})\sinh(\frac{3a_2}{2T}) + \exp(-4\frac{d}{T})\sinh(\frac{a_2}{2T})}{2\exp(\frac{2d}{T})\cosh(\frac{5a_2}{2T}) + 2\exp(-2\frac{d}{T})\cosh(\frac{3a_2}{2T}) + 2\exp(-4\frac{d}{T})\cosh(\frac{a_2}{2T})}, \tag{7}$$

where $a_2 = z_1 m_\sigma + \frac{J_b}{|J_{ab}|} z_3 m_s + h_0\cos(\xi)$. Hence, a set of mean-field dynamical equations for the system are obtained. We fixed $J_{ab} = -1$ that the intersublattice interaction is antiferromagnetic and $\Omega = 2\pi$. In the next section, we will give the numerical results of these equations.

3 Numerical Results and Discussions

3.1 Time Variations of Average Order Parameters

In this section, first we study the time variations of the average sublattice magnetizations to find the phases in the system. In order to investigate the behaviors of time variations of the average sublattice magnetizations, first, we have to study the stationary solutions of the set of coupled mean-field dynamical equations, given in (6) and (7), when the parameters T, J_a, J_b, d and h_0 are varied. The stationary solutions of these equations will be a periodic function of ξ with period 2π; that is, $m_\sigma(\xi + 2\pi) = m_\sigma(\xi)$ and $m_S(\xi + 2\pi) = m_S(\xi)$. Moreover, they can be one of three types according to whether they have or do not have the properties

$$m_\sigma(\xi + \pi) = -m_\sigma(\xi) \quad \text{and} \quad m_S(\xi + \pi) = -m_S(\xi). \tag{8}$$

The first type of solution which satisfies (8) is called a symmetric solution. It corresponds to a paramagnetic (p) phase. In this solution, the average sublattice magnetizations $m_\sigma(\xi)$ and $m_S(\xi)$ are equal to each other. They oscillate around the zero value and are delayed with respect to the external magnetic field. The second type of solution which does not satisfy (8), is called a nonsymmetric solution, and it corresponds to a ferromagnetic solution. In this solution, the submagnetizations $m_\sigma(\xi)$ and $m_S(\xi)$ are equal to each other ($m_\sigma(\xi) = m_S(\xi) \neq 0$). In this case, submagnetizations do not follow the external magnetic field any more, and instead of oscillating around zero, they oscillate around nonzero values, namely either $\pm 3/2$ or $\pm 1/2$; hence, we have the antiferromagnetic phase. If $m_\sigma(\xi)$ and $m_S(\xi)$ oscillate around $\pm 3/2$ and $\mp 3/2$ respectively, this solution is called the antiferromagnetic-3/2 ($\mathrm{af}_{3/2}$) phase. If $m_\sigma(\xi)$ and $m_S(\xi)$ oscillate around $\pm 1/2$ and $\mp 1/2$ respectively, this solution is called the

antiferromagnetic-1/2 ($af_{1/2}$) phase. The third type of solution, which does not satisfy (8), is also called a nonsymmetric solution, but this solution corresponds to a ferrimagnetic (i) solution because the submagnetizations $m_\sigma(\xi)$ and $m_S(\xi)$ are not equal to each other ($m_\sigma(\xi) \neq m_S(\xi)$), and they oscillate around a nonzero value. Hence, if $m_\sigma(\xi)$ and $m_S(\xi)$ oscillate around $\pm 3/2$ and $\mp 5/2$ respectively, this solution is called the ferrimagnetic-1 (i_1) phase. If $m_\sigma(\xi)$ and $m_S(\xi)$ oscillate around $\pm 3/2$ and $\mp 1/2$ respectively, the solution is called the ferrimagnetic-2 (i_2) phase. These facts are seen clearly by solving (6) and (7) using the Adams-Moulton predictor-corrector method for a given set of parameters and initial values. Since solutions to these kinds of equations are examined extensively in [21, 31, 47, 51], we will not discuss the solutions or present any figures here. From these studies, we observe that the system contains the p, $af_{3/2}$, $af_{1/2}$, i_1 and i_2 fundamental phases and the i_1 + p, $af_{3/2}$ + p, $af_{1/2}$ + p coexistences or mixed phases.

3.2 Thermal Behavior of the Dynamic Sublattice and Total Magnetizations

In this subsection, we investigate the temperature dependence of the dynamic sublattice magnetizations and the total dynamic magnetization to determine the DPT points and the compensation temperatures, respectively. This investigation leads us to characterize the nature (continuous and discontinuous) of dynamic transitions. The dynamic sublattice magnetizations (M_σ, M_S) and the dynamic total magnetization $M_t = (M_\sigma + M_S)/2$ are defined as

$$M_{\sigma,S} = \frac{1}{2\pi} \int_0^{2\pi} m_{\sigma,S}(\xi)\, d\xi, \tag{9}$$

and

$$M_t = \frac{1}{2\pi} \int_0^{2\pi} \left(\frac{m_\sigma(\xi) + m_S(\xi)}{2} \right) d\xi. \tag{10}$$

The behaviors of the dynamic sublattice magnetizations (M_σ, M_S) and the dynamic total magnetization (M_t) as functions of the temperature for several values of interaction parameters are obtained by solving (9) and (10). We solve these equations by combining the numerical methods of the Adams-Moulton predictor corrector with the Romberg integration. The dynamic total magnetization (M_t) vanishes at the compensation temperature T_{comp}. The compensation point can then be determined by looking for the crossing point between the absolute values of the sublattice magnetizations. Therefore, at the compensation point, we must have

$$|M_\sigma(T_{\text{comp}})| = |M_S(T_{\text{comp}})|, \tag{11}$$

and

$$\text{sgn}[M_\sigma(T_{\text{comp}})] = \text{sgn}[M_S(T_{\text{comp}})]. \tag{12}$$

We also require that $T_{\text{comp}} < T_{\text{C}}$, where T_{C} is the critical point temperature. A few explanatory and interesting examples are plotted in Figs. 1(a)–(c) in order to illustrate the calculation of the DPT points and the compensation temperatures. In these figures, T_{C} and T_t are the second- and first-order phase transition temperatures, respectively. T_{comp} is the compensation temperature. Figure 1(a) shows the behavior of $|M_\sigma|$, $|M_S|$ and $|M_t|$ as functions of the temperature for $J_{ab} = -1.0$, $J_a = 5.0$, $J_b = 0.2$, $d = 1.0$ and $h_0 = 0.1$. In this figure,

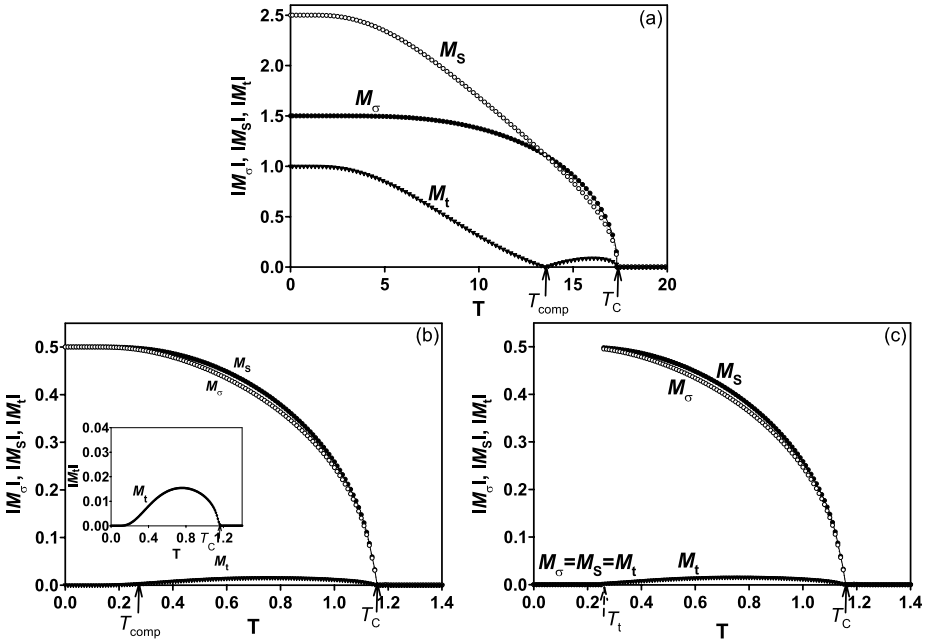

Fig. 1 The temperature dependence of the dynamic magnetizations ($|M_\sigma|$, $|M_S|$) and the dynamic total magnetization ($|M_t|$). T_C and T_t are the second- and first-order phase transition temperatures, respectively. T_{comp} is the compensation temperature. (**a**) Exhibiting a second-order phase transition from the i_1 phase to the p phase for $J_{ab} = -1.0$, $J_a = 5.0$, $J_b = 0.2$, $d = 1.0$ and $h_0 = 0.1$, and T_C is found to be 17.32. (**b**) Exhibiting a second-order phase transition from the $af_{1/2}$ phase to the p phase for $J_{ab} = -1.0$, $J_a = 1.1$, $J_b = 0.9$, $d = -3.5$ and $h_0 = 2.0$ and the initial values of $|M_\sigma|$ and $|M_S|$ are taken as 3/2 and 5/2, respectively; T_C is found to be 1.16. (**c**) Exhibiting two successive phase transitions, the first one is a first-order phase transition from the p phase to the $af_{1/2}$ phase, and the second one is a second-order phase transition the from the $af_{1/2}$ phase to the p phase for $J_{ab} = -1.0$, $J_a = 1.1$, $J_b = 0.9$, $d = -3.5$ and $h_0 = 2.0$ and the initial values of $|M_\sigma|$ and $|M_S|$ are taken as zero; T_C and T_t are found to be 1.16 and 0.26, respectively

$|M_\sigma| = 1.5$ and $|M_S| = 2.5$ are at zero temperature, and they decrease to zero continuously until T_C as the temperature increases; hence a second-order phase transition occurs at $T_C = 17.32$. In this case, the dynamic phase transition is from the i_1 phase to the p phase. Moreover, one compensation temperature or N-type behavior occurs in the system that exhibits the same behavior as that classified in the Néel theory [52] as the N-type behavior [53]. Figures 1(b) and 1(c) illustrate the thermal variations of $|M_\sigma|$, $|M_S|$ and $|M_t|$ for $J_{ab} = -1.0$, $J_a = 1.1$, $J_b = 0.9$, $d = -3.5$ and $h_0 = 2.0$ for various different initial values. $|M_\sigma| = 0.5$ and $|M_S| = 0.5$ at zero temperature, and they decrease to zero continuously until T_C as the temperature increases; hence a second-order phase transition occurs at $T_C = 1.16$. In this case, the dynamic phase transition is from the $af_{1/2}$ phase to the p phase. In Fig. 1(c), the system undergoes two successive phase transitions: The first one is a first-order phase transition because a discontinuity occurs for the dynamic sublattice magnetizations at $T_t = 0.26$. The transition is from the p phase to the $af_{1/2}$ phase. The second is a second-order phase transition from the $af_{1/2}$ phase to the p phase at $T_C = 1.16$. This means that the coexistence region, i.e., the $af_{1/2}$ + p mixed phase, exists in the system, and this fact is seen clearly in the phase diagram of Fig. 3(c) (compare in Figs. 1(b) and 1(c) with Fig. 3(c)). Moreover, one compensation temperature or L-type behavior occurs in the

system (see Fig. 1(b)) which exhibits the same behavior as that classified in the Néel theory [52] as the L-type behavior [53].

We also studied the compensation behavior of the system in detail and found that it exhibits the Q-, R-, P-, S-, N- and L-type behaviors that can be seen in Figs. 2(a)–(f), re-

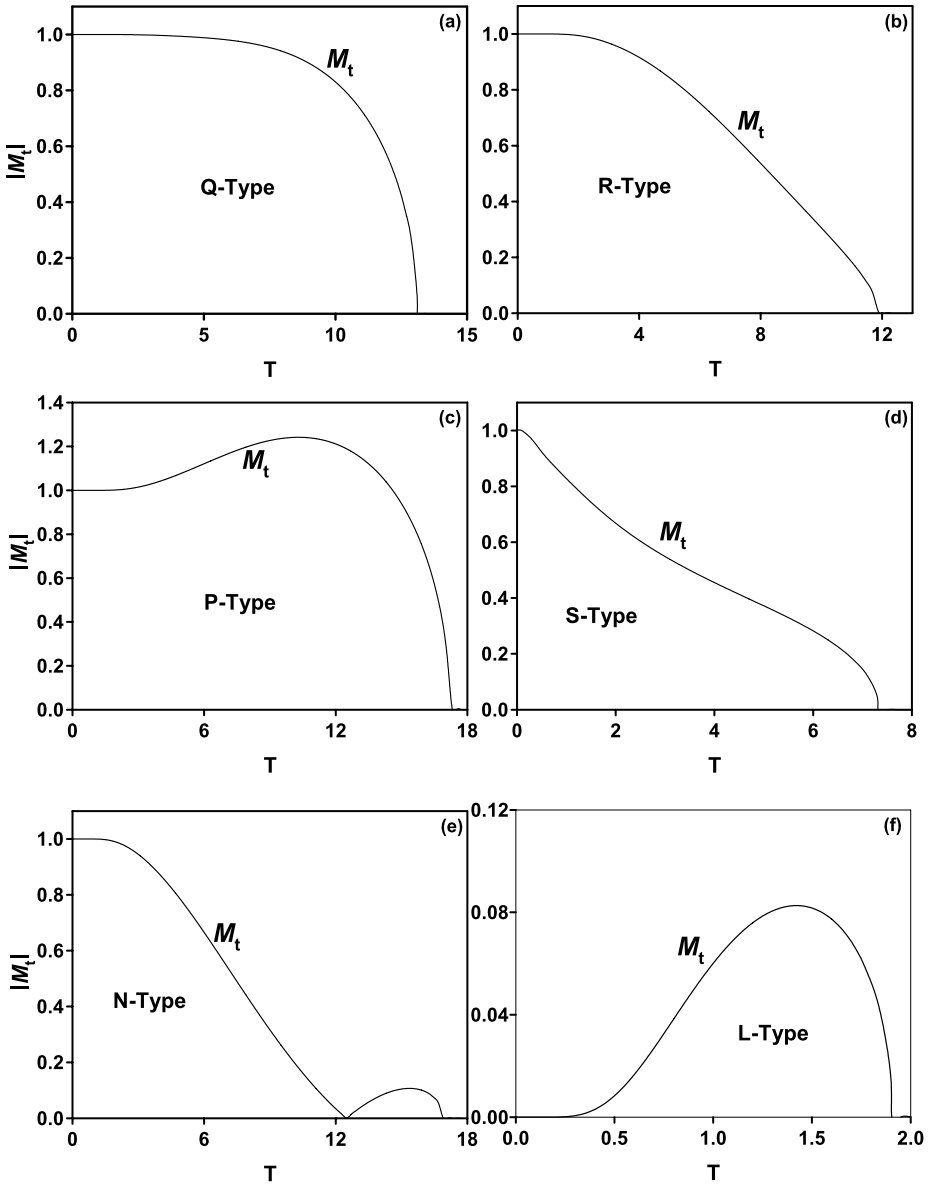

Fig. 2 The dynamic total magnetization as a function of the temperature for different values of interaction parameters. The system exhibits the Q-, R-, P-, S-, N- and L-types of compensation behaviors. (**a**) $J_{ab} = -1.0$, $J_a = 1.1$, $J_b = 0.9$, $d = 1.0$ and $h_0 = 1.0$, (**b**) $J_{ab} = -1.0$, $J_a = 2.0$, $J_b = 0.1$, $d = 1.0$ and $h_0 = 1.0$, (**c**) $J_{ab} = -1.0$, $J_a = 0.2$, $J_b = 2.0$, $d = 1.0$ and $h_0 = 1.0$, (**d**) $J_{ab} = -1.0$, $J_a = 1.1$, $J_b = 0.1$, $d = -2.0$ and $h_0 = 2.0$, (**e**) $J_{ab} = -1.0$, $J_a = 5.0$, $J_b = 0.2$, $d = 0.5$ and $h_0 = 0.1$, (**f**) $J_{ab} = -1.0$, $J_a = 2.0$, $J_b = 0.8$, $d = -4.0$ and $h_0 = 1.0$

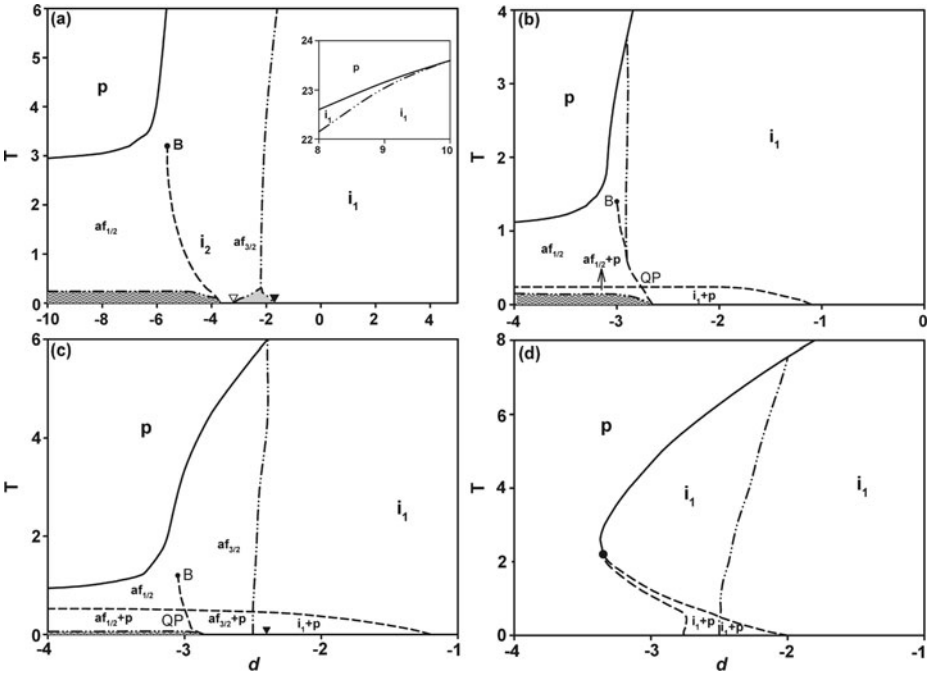

Fig. 3 Dynamic phase diagrams of the mixed spin Ising ferrimagnetic model in the (d, T) plane. *Solid*, *dashed* and *dash-dot-dot lines* are the dynamic second-, first-order phase transitions and the compensation temperature lines, respectively. The special points are the dynamic tricritical point (●), double critical end point (B), quadruple point (QP). The filled (▲) and unfilled (△) triangles correspond to the separation points which separate the ferrimagnetic-1 (i_1) phase from the antiferromagnetic-3/2 ($af_{3/2}$) phase, and the $af_{3/2}$ phase from the ferrimagnetic-2 (i_2) phase, respectively. (**a**) $J_{ab} = -1.0$, $J_a = 5.0$, $J_b = 0.2$ and $h_0 = 0.1$, (**b**) $J_{ab} = -1.0$, $J_a = 2.0$, $J_b = 0.8$ and $h_0 = 1.0$, (**c**) $J_{ab} = -1.0$, $J_a = 1.1$, $J_b = 0.9$ and $h_0 = 2.0$, (**d**) $J_{ab} = -1.0$, $J_a = 1.5$, $J_b = 0.5$ and $h_0 = 2.2$

spectively. These behaviors depend strongly on the interaction parameter. We should also mention that the M- and W-type curves cannot appear in the system.

3.3 Dynamic Phase Diagrams

Since we obtained DPT points and compensation temperatures in Sect. 3.2, we can now present the dynamic phase diagrams of the system. The phase diagrams calculated in the (d, T) plane are presented in Fig. 3 and one explanatory phase diagram for each of the (J_a, T), $(-J_b, T)$, (d, J_a) and $(d, -J_b)$ planes is presented, seen in Figs. 4(a)–(d) for various values of interaction parameters, respectively. In these dynamic phase diagrams, the dashed, solid and dash-dot-dot lines represent the first-order, second-order phase transitions temperatures and the compensation temperatures, respectively. The special points are the dynamic tricritical point with a filled circle, the double critical end point (B), the triple point (TP), the quadruple point (QP) and separating point depicted as the filled and unfilled triangles. The hatched regions shown in grey are the $af_{3/2}$ phase, and the hatched regions with the zigzag lines are the $af_{1/2}$ phase where the compensation effect exists in both regions; hence the total magnetizations vanish in these regions.

Figure 3 illustrates the dynamic phase diagrams in the (d, T) plane for various values of the interaction parameters, and eight main distinct topological types of phase diagrams are

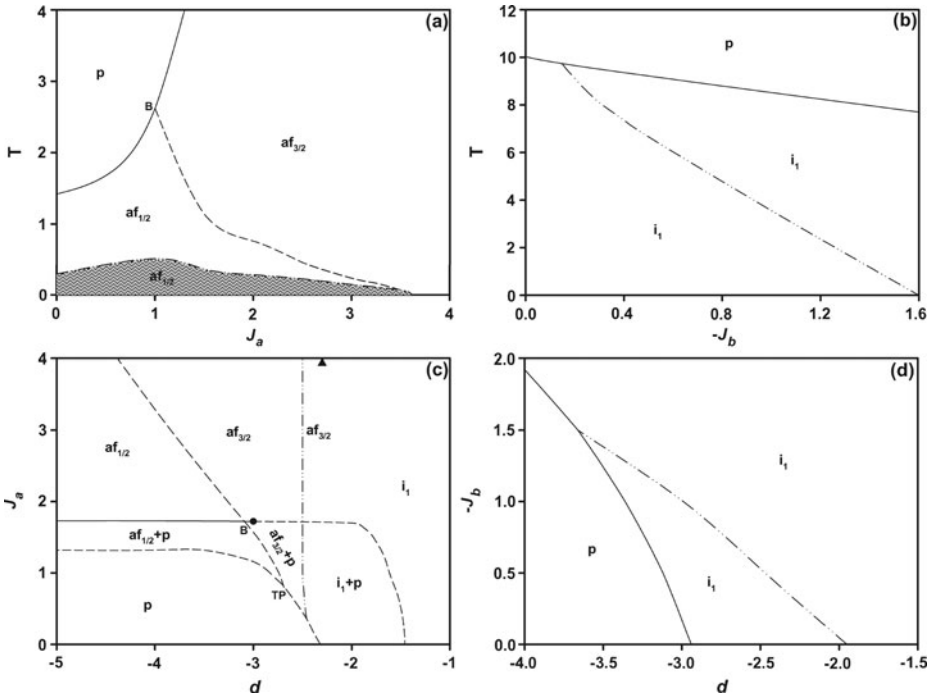

Fig. 4 Same as Fig. 3, but in different planes. TP is the dynamic triple point. (**a**) In (J_a, T) plane for $J_{ab} = -1.0$, $J_b = 0.9$, $d = -3.0$ and $h_0 = 0.1$. (**b**) In $(-J_b, T)$ plane for $J_{ab} = -1.0$, $J_a = 2.0$, $d = -0.5$ and $h_0 = 0.1$. (**c**) In (d, J_a) plane for $J_{ab} = -1.0$, $J_b = 0.5$, $T = 0.3$ and $h_0 = 2.2$, the *filled triangle* corresponds to the separation points which separate the i_1 phase from the $af_{3/2}$ phase. (**d**) In $(d, -J_b)$ plane for $J_{ab} = -1.0$, $J_a = 1.5$, $T = 2.0$ and $h_0 = 2.2$

found. We only present four representative and more interesting graphs. From these phase diagrams, the following interesting phenomena and main results are observed.

(i) The phase diagrams contain the compensation temperatures.
(ii) Figure 3(d) exhibits a reentrant behavior, i.e., as the temperature is increased, the system passes from the paramagnetic (p) phase to the ordered phases, and back to the p phase again.
(iii) The phase diagrams of Fig. 3(d), Figs. 3(a)–(c) and Figs. 3(b)–(c) display the dynamic tricritical, the double critical end (B), and the dynamic quadrupole (QP) points, respectively.
(iv) The system contains the p, $af_{3/2}$, $af_{1/2}$, i_1 and i_2 fundamental phases and the $i_1 + p$, $af_{3/2} + p$, $af_{1/2} + p$ coexistences or mixed phases.
(v) The dynamic phase boundaries among the fundamental phases are mostly a second-order phase transition lines, but among the mixed phases or between the fundamental and mixed phases are mostly first-order phase transition lines.

We also calculated the dynamic phase diagrams, including the compensation behaviors in the (J_a, T), $(-J_b, T)$, (d, J_a) and $(d, -J_b)$ planes, and five, five, eight and seven main distinct topological dynamic phase diagrams were found, respectively. Since most of the phase diagrams in these planes can be readily obtained from the phase diagrams in the (d, T)

plane, especially for very high and low values of d and T, we give only one interesting phase diagram in each plane, see Figs. 4(a)–(d).

Figure 4(a) is obtained for $J_{ab} = -1.0$, $J_b = 0.9$, $d = -3.0$ and $h_0 = 0.1$ in the (J_a, T) plane. The system exhibits one dynamic double critical end point (B) and the dynamic phase boundary between the $af_{1/2}$ and $af_{3/2}$ phases is always a first-order phase transition line. The dynamic phase boundaries between the $af_{1/2}$ and p phases, and between the $af_{3/2}$ and p phases are second-order phase transition lines. The hatched region with the zigzag lines is the $af_{1/2}$ phase where the compensation effect exists; hence the total dynamic magnetization vanishes. As we can see, a compensation effect disappears only when a maximum value of J_a is reached. Moreover, if one increases J_a values, the $af_{3/2}$ phase region becomes larger. We found a phase diagram similar to the one seen in the mixed spin-1/2 and spin-1 Ising system [44] and in the mixed spin-1/2 and spin-3/2 Ising model on a hexagonal lattice [47].

Figure 4(b) is calculated for $J_{ab} = -1.0$, $J_a = 2.0$, $d = -0.5$ and $h_0 = 0.1$ in the $(-J_b, T)$ plane. As we can see, T_C and T_{comp} are both decreasing functions of J_b. These results were expected because as J_b increases, M_S decreases, and a lower temperature is needed for which $M_\sigma = M_S$. At a given value of J_b, the compensation temperature goes to zero. We found a similar phase diagram to the one seen in the mixed spin-1/2 and spin-1 Ising system [44] and in the mixed spin-1 and spin-3/2 Ising system [54].

For $J_{ab} = -1.0$, $J_b = 0.5$, $T = 0.3$ and $h_0 = 2.2$, the phase diagram in the (d, J_a) plane is presented in Fig. 4(c). One can observe that this phase diagram contains the p, $af_{3/2}$, $af_{1/2}$, and i_1 fundamental phases and the i_1+ p, $af_{3/2}$ + p, $af_{1/2}$ + p coexistences or mixed phases. The dynamic phase boundaries among these phases are mostly first-order phase transition lines, except the boundaries between the $af_{1/2}$ and $af_{1/2}$ + p phases, between the $af_{3/2}$ and $af_{3/2}$ + p phases for certain values of d. Moreover, this figure displays a dynamic tricritical point, double critical end point (B), triple point (TP) and separating point (▲). The filled triangle corresponds to the separating point which separates the $af_{3/2}$ phase from the ferrimagnetic-1 (i_1) phase. As we can see, a compensation point appears only when a minimum value of J_a is reached. As to be expected, increasing J_a above its minimum value, the first magnetization M_σ keeps ordered up to a high value of crystal-field. However, M_S is almost constant, the crossing point between M_σ and M_S changes a little, and the compensation value is nearly constant.

Finally, Fig. 4(d) is constructed for $J_{ab} = -1.0$, $J_a = 1.5$, $T = 2.0$ and $h_0 = 2.2$ in the $(d, -J_b)$ plane. The p and i_1 fundamental phases occur in the system, and the dynamic phase boundary between these phases is only a second-order phase transition line. Moreover, this figure contains the compensation temperature, but does not exhibit any dynamic critical point. As we can see, T_C and T_{comp} are both decreasing functions of d. These results were expected because as J_b increases, M_S decreases, and a lower temperature is needed for which $M_\sigma = M_S$. At a given value of d, the compensation temperature goes to zero.

4 Summary and Conclusion

In this work, we have studied within a mean-field approach the stationary states of the kinetic mixed spin-3/2 and spin-5/2 ferrimagnetic Ising model in the presence of a time-dependent oscillating external magnetic field on a hexagonal lattice. The model consists of two interpenetrating sublattices with $\sigma = 3/2$ and $S = 5/2$. For this spin arrangement, any spin at one lattice site has two nearest-neighbor spins on the same sublattice, and four on the other sublattice. The Hamiltonian model includes the intersublattice interaction, intrasublattice interaction, crystal field interaction and sinusoidal magnetic field. The intersublattice interaction is antiferromagnetic. We use the Glauber-type stochastic dynamics to describe the

time evolution of the system. We have studied time variations of the average magnetizations in order to find the phases in the system and the temperature dependence of the average magnetizations in a period, which is also called the dynamic magnetizations, to obtain the dynamic phase transition (DPT) points as well as to characterize the nature (continuous or discontinuous) of transitions. The total dynamic magnetization is investigated as a function of temperature to find the compensation temperatures and to determine the type of behavior. Finally, dynamic phase diagrams are presented in five different planes. The phase diagrams contain the paramagnetic (p), antiferromagnetic-1/2 ($af_{1/2}$), antiferromagnetic-3/2 ($af_{3/2}$), ferrimagnetic-1 (i_1), ferrimagnetic-2 (i_2) phases, the $af_{1/2} + p$, $af_{3/2} + p$ and $i_1 + p$ mixed phases, and the compensation temperatures or Q-, R-, P-, S-, N- and L-type behaviors in the Néel classification nomenclature, depending on the interaction parameters. The system also displays the dynamic tricritical point, double critical end point, triple point, quadruple point, separating point and reentrant behavior, which also strongly depend on interaction parameters. Moreover, in general, the dynamic phase boundaries among the fundamental phases are second-order lines, but the boundaries between the fundamental and mixed phases and among the mixed phases are first-order lines.

Finally, we should also mention that this mean-field dynamic study, in spite of its limitations, such as the correlation of spin fluctuations have not been considered, suggests that the kinetic mixed spin-3/2 and spin-5/2 ferrimagnetic Ising model has an interesting dynamic behavior and provides rich dynamic phase diagrams as well as the dynamic compensation behaviors. Hence, we hope that our detailed theoretical investigation may stimulate further works to study the nonequilibrium or the dynamic phase transition in the kinetic mixed spin-3/2 and spin-5/2 ferrimagnetic Ising model by using more accurate techniques such as kinetic Monte-Carlo simulations or the renormalization-group calculation. We also hope that our results will be instructive in the time consuming process of researching critical behavior of this system using the dynamic MC simulations.

Acknowledgements This work was supported by the Scientific and Technological Research Council of Turkey (TÜBİTAK) Grant No: 107T533 and Erciyes University Research Funds Grant No: FBA-06-01 and FBD-08-593. One of us (B.D.) would like to express his gratitude to the TÜBİTAK for Ph.D. scholarship.

References

1. Li, P.F., Chen, Y.G., Chen, H.: Second- to first-order transition in two coupled antiferromagnetic rings. Eur. Phys. J. B **51**, 473 (2006)
2. Bobák, A., Jurčišin, M.: Ferrimagnetism in diluted mixed-spin two-dimensional Ising models. J. Magn. Magn. Mater. **163**, 292 (1996)
3. Buendía, G.M., Cardona, R.: Monte Carlo study of a mixed spin-3/2 and spin-1/2 Ising ferrimagnetic model. Phys. Rev. B **59**, 6784 (1999)
4. Jiang, W., Wei, G.-Z., Xin, Z.-H.: Magnetic properties of a mixed spin-1/2 and spin-3/2 transverse Ising model with a crystal field. Physica A **293**, 455 (2001)
5. Wei, G.-Z., Liang, Y.-Q., Zhang, Q., Xin, Z.-H.: Magnetic properties of mixed-spin Ising systems in a longitudinal magnetic field. J. Magn. Magn. Mater. **271**, 246 (2004)
6. Li, J., Wei, G., Du, A.: Green function study of a mixed spin-3/2 and spin-1/2 Heisenberg ferrimagnetic model. J. Magn. Magn. Mater. **269**, 410 (2004)
7. Ekiz, C.: Mixed spin-1/2 and spin-3/2 Ising system in a longitudinal magnetic field. J. Magn. Magn. Mater. **293**, 913 (2005)
8. Jaščur, M., Strečka, J.: Magnetic properties of a mixed spin-1/2 and spin-3/2 Ising model with an uniaxial and biaxial crystal-field potential. Physica A **358**, 393 (2005)
9. Zhang, X., Kong, X.-M.: Ferromagnetism in the mixed spin-1/2 and spin-3/2 Blume-Capel system on the two-fold Cayley tree. Physica A **369**, 589 (2006)
10. Essaoudi, I., Bärner, K., Ainane, A., Saber, M.: Magnetic properties and hysteresis loops of the $S = 1/2$ and $S = 3/2$ bilayer Ising model. Physica A **385**, 208 (2007)

11. Liang, Y.-Q., Wei, G.-Z., Ma, F.-C., Song, G.-L.: Magnetic properties of a mixed spin-1/2 and spin-3/2 transverse Ising model in a longitudinal magnetic field. Physica A **387**, 4513 (2008)
12. Deviren, B., Keskin, M., Canko, O.: Kinetics of a mixed spin-1/2 and spin-3/2 Ising ferrimagnetic model. J. Magn. Magn. Mater. **321**, 458 (2009)
13. Deviren, B., Keskin, M., Canko, O.: Magnetic properties of an anti-ferromagnetic and ferrimagnetic mixed spin-1/2 and spin-5/2 Ising model in the longitudinal magnetic field within the effective-field approximation. Physica A **388**, 1835 (2009)
14. Strečka, J.: Exact results of a mixed spin-1/2 and spin-S Ising model on a bathroom tile (4–8) lattice: effect of uniaxial single-ion anisotropy. Physica A **360**, 379 (2006)
15. Zhang, Q., Wei, G.-Z., Gu, Y.: The study of the phase diagram and internal energy of the mixed spin-3/2 and spin-5/2 ferrimagnetic Ising system with interlayer coupling by effective-field theory; a simple approach of calculating internal energy. Phys. Status Solidi B **242**, 924 (2005)
16. Albayrak, E., Yiğit, A.: Mixed spin-3/2 and spin-5/2 Ising system on the Bethe lattice. Phys. Lett. A **353**, 121 (2006)
17. Yessoufou, R.A., Amoussa, H.S., Hontinfinde, F.: Magnetic properties of the mixed spin-5/2 and spin-3/2 Blume-Capel Ising system on the two-fold Cayley tree. Cent. Eur. J. Phys. **7**, 555 (2009)
18. De la Espriella, N., Buendía, G.M.: Ground state phase diagrams for the mixed Ising 3/2 and 5/2 spin model. Physica A **389**, 2725 (2010)
19. Bellessa, G.: High-spin tunneling in Fe-8 molecular magnets. Europhys. Lett. **52**, 358 (2000)
20. Buendía, G.M., Machado, E.: Kinetics of a mixed Ising ferrimagnetic system. Phys. Rev. E **58**, 1260 (1998)
21. Keskin, M., Kantar, E., Canko, O.: Kinetics of a mixed spin-1 and spin-3/2 Ising system under a time-dependent oscillating magnetic field. Phys. Rev. E **77**, 051130 (2008)
22. Keskin, M., Canko, O., Guldal, S.: Phase diagrams of a nonequilibrium mixed spin-1/2 and spin-2 Ising ferrimagnetic system under a time-dependent oscillating magnetic field. Phys. Lett. A **374**, 1 (2009)
23. Maltempo, M.M., Moss, T.H.: The spin 3/2 state and quantum spin mixtures in haem proteins. Rev. Biophys. **9**, 181 (1976)
24. Dugad, L.B., Marathe, V.R., Mitra, S.: Electronic-structure of spin-mixed iron(III) porhyrins—a proton magnetic-resonance study. Proc. Indian Acad. Sci. **95**, 189 (1985)
25. Weiss, R., Gold, A., Terner, J.: Cytochromes c′: biological models for the $S = 3/2$, 5/2 spin-state admixture? Chem. Rev. **106**, 2550 (2006)
26. Zeng, Y., Caignan, G.A., Bunce, R.A., Rodriguez, J.C., Wilks, A., Rivera, M.: Azide-inhibited bacterial heme oxygenases exhibit an $S = 3/2$ $(d_{xz}, d_{yz})^3(d_{xy})^1(d_z^2)^1$ spin state: mechanistic implications for heme oxidation. J. Am. Chem. Soc. **127**, 9794 (2005)
27. Rakow, N.A., Suslick, K.S.: A colorimetric sensor array for odour visualization. Nature **406**, 710 (2000)
28. Glauber, R.J.: Time-dependent statistics of the Ising model. J. Math. Phys. **4**, 294 (1963)
29. Chakrabarti, B.K., Acharyya, M.: Dynamic transitions and hysteresis. Rev. Mod. Phys. **71**, 847 (1999)
30. Sides, S.W., Rikvold, P.A., Novotny, M.A.: Kinetic Ising model in an oscillating field: finite-size scaling at the dynamic phase transition. Phys. Rev. Lett. **81**, 834 (1998)
31. Keskin, M., Canko, O., Deviren, B.: Dynamic phase transition in the kinetic spin-3/2 Blume-Capel model under a time-dependent oscillating external field. Phys. Rev. E **74**, 011110 (2006)
32. Robb, D.T., Rikvold, P.A., Berger, A., Novotny, M.A.: Conjugate field and fluctuation-dissipation relation for the dynamic phase transition in the two-dimensional kinetic Ising model. Phys. Rev. E **76**, 021124 (2007)
33. Samoilenko, Z.A., Okunev, V.D., Pushenko, E.I., Isaev, V.A., Gierlowski, P., Kolwas, K., Lewandowski, S.J.: Dynamic phase transition in amorphous YBaCuO films under Ar laser irradiation. Inorg. Mater. **39**, 836 (2003)
34. Jiang, Q., Yang, H.-N., Wang, G.C.: Scaling and dynamics of low frequency hysteresis loops in ultrathin Co films on a Cu(001) surface. Phys. Rev. B **52**, 14911 (1995)
35. Kleemann, W., Braun, T., Dec, J., Petracic, O.: Dynamic phase transitions in ferroic systems with pinned domain walls. Phase Transit. **78**, 811 (2005)
36. Gedik, N., Yang, D.-S., Logvenov, G., Bozovic, I., Zewail, A.H.: Nonequilibrium phase transitions in cuprates observed by ultrafast electron crystallography. Science **316**, 425 (2007)
37. Robb, D.T., Xu, Y.H., Hellwig, O., McCord, J., Berger, A., Novotny, M.A., Rikvold, P.A.: Evidence for a dynamic phase transition in $[Co/Pt]_3$ magnetic multilayers. Phys. Rev. B **78**, 134422 (2008)
38. Kanuga, K., Cakmak, M.: Dynamic phase diagram derived from large deformation non-linear mechano-optical behavior of polyethylene naphthalate nanocomposites. Polymer **48**, 7176 (2007)
39. Mansuripur, M.: Magnetization reversal, coercivity, and the process of thermomagnetic recording in thin-films of amorphous rare-earth transition-metal alloys. J. Appl. Phys. **61**, 1580 (1987)
40. Mathoniere, C., Nuttall, C.J., Carling, S.G., Day, P.: Ferrimagnetic mixed-valency and mixed-metal tris(oxalato)iron(III) compounds: Synthesis, structure, and magnetism. Inorg. Chem. **35**, 1201 (1996)

41. Hernando, A., Kulik, T.: Exchange interaction through amorphous paramagnetic layers in ferromagnetic nanocrystals. Phys. Rev. B **49**, 7064 (1994)
42. Alex, M., Shono, K., Kuroda, S., Koshino, N., Ogawa, S.: Ce-substituted garnet media for magnetooptic recording. J. Appl. Phys. **67**, 4432 (1990)
43. Machado, E., Buendía, G.M.: Metastability and compensation temperatures for a mixed Ising ferrimagnetic system. Phys. Rev. B **68**, 224411 (2003)
44. Godoy, M., Leite, V.S., Figueiredo, W.: Mixed-spin Ising model and compensation temperature. Phys. Rev. B **69**, 054428 (2004)
45. Keskin, M., Ertas, M.: Mixed-spin Ising model in an oscillating magnetic field and compensation temperature. J. Stat. Phys. **139**, 333 (2010)
46. Leite, V.S., Godoy, M., Figueiredo, W.: Finite-size effects and compensation temperature of a ferrimagnetic small particle. Phys. Rev. B **71**, 094427 (2005)
47. Keskin, M., Deviren, B., Canko, O.: Dynamic compensation temperature in the mixed spin-1/2 and spin-3/2 Ising model in an oscillating field on alternate layers of hexagonal lattice. IEEE Trans. Magn. **45**, 2640 (2009)
48. Keskin, M., Ertas, M.: Existence of a dynamic compensation temperature of a mixed spin-2 and spin-5/2 Ising ferrimagnetic system in an oscillating field. Phys. Rev. E **80**, 061140 (2009)
49. Chern, G., Horng, L., Shieh, W.K., Wu, T.C.: Antiparallel state, compensation point, and magnetic phase diagram of Fe_3O_4/Mn_3O_4 superlattices. Phys. Rev. B **63**, 094421 (2001)
50. Kageyama, H., Khomskii, D.I., Levitin, R.Z., Vasil'ev, A.N.: Weak ferrimagnetism, compensation point, and magnetization reversal in $Ni(HCOO)_2$ center dot $2H_2O$. Phys. Rev. B **67**, 224422 (2003)
51. Temizer, Ü., Keskin, M., Canko, O.: Dynamic compensation temperature in the kinetic spin-1 Ising model in an oscillating external magnetic field on alternate layers of a hexagonal lattice. J. Magn. Magn. Mater. **321**, 2999 (2009)
52. Néel, L.: Magnetic properties of ferrites: ferrimagnetism and antiferromagnetism. Ann. Phys. **3**, 137 (1948)
53. Chikazumi, S.: Physics of Ferromagnetism. Oxford University Press, Oxford (1997)
54. Keskin, M., Kantar, E.: Dynamic compensation temperatures in the mixed spin-1 and spin-3/2 Ising system under a time-dependent oscillating magnetic field. J. Magn. Magn. Mater. **322**, 2789 (2010)